ISTITUTO NAZIONALE DI FISICA NUCLEARE

Sezione di Trieste

INFN/AE-93/20

9 novembre 1993

G.Barbiellini, M. Boezio, A. Rindi and C. Rizzo

MONTE CARLO STUDY OF A POSITRON EMISSION TOMOGRAPH BASED ON MULTISTRIP MULTILAYER Si DETECTORS

Servizio Documentazione
dei Laboratori Nazionali di Frascati

Monte Carlo study of a Positron Emission Tomograph based on multistrip multilayer Si detectors.

M.Boezio, C.Rizzo
Istituto Nazionale di Fisica Nucleare, Sezione di Trieste, Laboratori - Area di Ricerca,
Padriciano 99, I-34012 Trieste, Italy

G. Barbiellini
Dipartimento di Fisica dell'Università di Trieste
and
Istituto Nazionale di Fisica Nucleare, Sezione di Trieste,
Via A. Valerio 2, I-34127 Trieste, Italy

A.Rindi
Società Sincrotrone Trieste, Area di Ricerca,
Padriciano 99, I-34012 Trieste, Italy

(Submitted to Physica Medica)

Abstract

We have simulated a Positron Emission Tomograph based on the use of multistrip multilayer Silicon detectors with a depleted Uranium 40 μm thick converters. The imaging capabilities of the tomograph have been studied with a fully 3-D Monte Carlo simulation based on the GEANT code. By using a simple 3-D back projection algorithm a spatial resolution of about 2 mm (Full Width Half Maximum) has been obtained with a ^{18}F point source.

1. Introduction

Positron Emission Tomography (PET) [1] is based on the idea that by detecting the two 511 keV gammas produced by a positron annihilating in the tissue one can sample a β^+ emitter distribution in a biological target.

This imaging technique was first suggested by Wren and co-workers [2] and Sweet [3], and first prototype scanner was built by Brownell and Sweet [4] using as gamma detectors two NaI crystal scintillators. The volume scanned by the detection of the two annihilation gammas is limited by the active surface of the two coincidence detectors. The original radioisotope distribution is reconstructed by a series of "projection" obtained by rotating the detectors around the biological sample.

Many physical processes are involved in the detection in coincidence of the two annihilation photons.

In table 1 we list the mostly used positron emitters, together with the lifetime and the mean energy of the β^+ spectrum [5]; ^{11}C, ^{13}N, ^{15}O, ^{18}F are particularly attractive for physiological study.

Table 1 - Positron emitters most used in PET

Radioisotope	$\tau_{\frac{1}{2}}$ (minutes)	Mean energy of β^+ spectrum T_{mean} (MeV)
^{11}C	20.4	0.385
^{13}N	10.0	0.491
^{15}O	2.0	0.735
^{18}F	109.8	0.242
$(^{82}Sr) \Rightarrow {}^{82}Rb$	1.3	1.410
$(^{68}Ge) \Rightarrow {}^{68}Ga$	68.1	0.740

Before annihilating the positron travels a finite range, which depends upon its energy (see table 1). The range in tissue for ^{18}F, which has the lowest mean energy, is about 1 mm [6]. The annihilation of a positron with an electron, both at rest, would imply

the emission of two gammas in opposite directions. However, due to Fermi motion, the distribution of the angle between the direction of the two emitted photons is almost gaussian around 180°. In water, and therefore in biological tissues which are mainly constituted by water, the σ of the distribution is about 0.3° [7]. Moreover, since the mean free path of a 511 keV gamma in water is about 8.5 cm, for a standard 20 cm size biological region of interest only 30 % of the two gammas will reach the detectors unaffected by the Compton scattering. Furthermore the fraction of the scattered photons will still produce coincidence events smearing the resolution and decreasing the contrast of the final image.

Finally, the detection of the two photons depends upon design physical parameters of the detectors. The most common commercially available tomographs are made by rings of bismuth germanate ($Bi_4Ge_3O_{12}$) crystal detectors. The improvement achievable with this kind of scintillators was demonstrated for the first time by a Montreal group on a tomograph for the head (POSITOMEII) [8].

For the design of a PET camera, the following requirements are important :

- a high detection efficiency for 511 keV gammas;
- a short temporal resolution for the coincidence;
- a high spatial resolution of the gamma detectors;
- a large solid angle coverage.

To finally obtain an image of the reconstructed radioisotope distribution a suitable computer is essential. It deals with acquisition of the data, mass storage and reconstruction of the images. Moreover the tendency is increasingly to present the image in 3-dimension. Most of the tomographs are intrinsically 2-dimensional, however in order to use all the emitted radiation there is a trend towards intrinsically 3-dimensional tomograph and intrinsically 3-dimensional reconstruction algorithm [9].

We have designed a non conventional Positron Emission Tomograph based on multistrip multilayer silicon detectors. In recent years multistrip silicon detectors have been widely used in different fields, from astroparticles physics [10] and colliders physics [11,12] to x rays detectors for medical purpose [13,14].
With this Monte Carlo simulation we studied the feasibility of their use, together with a thin converter layer, for the detection of 511 keV gammas for PET.

2. The tomograph design

The tomograph we designed is constituted by two detection modules that rotate around the biological region of interest as in the original Brownell and Sweet [4] scanner. Each module is composed by a stack of silicon detectors each one interlayered with a depleted uranium plane as gamma converter. Fig. 1 shows a schematic drawing of the tomograph.

As silicon detectors we focused our attention on the ones used in ref. 12 and 13. These are silicon strip detectors with readout strips on both sides of the same wafer for bidimensional position information for each particle hit. We assumed a 300 μm thickness of the detector and a 1 mm readout pitch on both of its sides. The active area was assumed to be 6 x 12 cm^2. This could be reached using two 6 x 6 cm^2 active area detectors per converter layer; connecting together the strips of the two detectors in one of the two coordinate one obtains 180 readout channels per layer. In conclusion if the total number of silicon detectors is about 100 we think that the complexity of the tomograph is less than the complexity of the ALEPH silicon strip vertex detector [12] which has been built for collider physics and is currently on data taking.

The use of a thin high Z converter layer increases the total efficiency of the module; depleted uranium has been considered because, for 511 keV gammas, the photoelectric cross section and the Compton cross section are high enough to obtain a good converter efficiency. In fig. 2 we show the total photon cross section for U and Si as given by the GEANT code [15] we used for the simulation.

Since after photon convertion the photoelectric or Compton electron produced must reach the silicon layer to be detected the thickness of the Uranium layer must be optimized in order to have the maximum convertion efficiency compatible with the highest probability for the electron produced to reach the silicon detector.

The design parameters have been set according to the Monte Carlo simulation.

3 The Monte Carlo simulation

3.1. The GEANT code [15]

For the 3-D simulation of the tomograph we have implemented a 3-D Monte Carlo program based on the GEANT code version 3.15 [15].

This code has been originally developed for high energy physics and it can simulate both electromagnetic and adronic showers. Its use in the case of a silicon detector calorimeter has been already tested [10] for a simulation very similar to ours and we used the same parameter optimization.

In particular we have set DEEMAX (maximum energy fraction that a particle can lose for ionization) = 0.05; STMIN (minimum tracking step) = 0.0005 cm; STEMAX (maximum tracking step) = 100.0 cm; EPSIL (tracking precision) = 1% of the size of every region simulated. Moreover we have chosen the explicit delta ray generation to simulate the fluctuations in the energy deposit. The cuts for the lowest energy have been set at 10 keV for both photons and electrons.

In the following we will give more details of every simulation step we have implemented to complete simulate the tomograph and to obtain simulate data to feed the reconstruction program.

3.2 Positron range

We have simulated a pointlike ^{18}F source embedded in a 24 cm size water phantom. The ^{18}F, compared to the other more commonly used isotopes (see Table 1), has the minimum range for the emitted positron. To take into account this range in water, following the experimental results shown in ref. 6, we applied to the original distribution of annihilation point a gaussian distribution of $\sigma = 0.049$ cm.

3.3 Gamma non collinearity

After the annihilation point the Monte Carlo program generate the direction in which the two annihilation photon are emitted. A couple of photons is simulated; to the first one we assign the momentum $\vec{P}_1$ coming from the random generate direction, to the second one we assign a momentum $\vec{P}_2$, equal to $\vec{P}_1$ in module but so that

$$\frac{\vec{P}_1 \bullet \vec{P}_2}{|P_1||P_2|} = \mathrm{Cos}(180° - \vartheta)$$

where ϑ is an angle whose distribution is a gaussian around 0° with $\sigma = 0.3°$ as suggested by ref. [7] to simulate gamma non collinearity in water.

3.4 The Si detectors with the U converter

Finally the photon coming out from the water phantom reaches the detector region. We assumed that an event has been detected if in the silicon region an energy greater than 20 keV has been deposited. This energy value has been chosen from experimental data shown in ref. [10] e ref. [12] to take into account the overall noise of the detector. The detection coordinates given by the silicon detectors will be finally used in the image reconstruction.

In fig. 3 we show the Monte Carlo result we have produced to optimize the converter layer thickness. For a reasonable number of 25 converter / silicon detector layers we have the maximum detection efficiency when the uranium thickness per each detector is about 40 μm.

In fig. 4 we see how the total efficiency increase increasing with the number of U/Si layers.

In principle one could obtain an efficiency close to 1 but to maintain the overall complexity of the tomograph at a reasonable level we assumed 25 U/Si layers per module corresponding to a total number of silicon detector of 100.

The photon hitting the detection module could be already Compton scattered by the water phantom; in fig. 5 we show the efficiency of the 25 U/Si layer module versus the incident gamma energy; we see that the use of converter layers introduces a cut in the efficiency with energy less than 300 keV decreasing the probability of coincidence between a 511 keV gamma and a Compton scattered gamma.

Simulation results confirm that the gamma deposes the energy, via convertion in the Uranium converter or compton scattering in the silicon, in a region of dimension less than the 1 mm pitch of the strips. It is possible, therefore, to determine unambigously the detection coordinate for any event.

From fig. 3 we can see that about 50 % of the detected events comes from photon directly interacting in the silicon detector without conversion in the converter. Since the cross section for 511 keV photon in silicon is mostly determined by Compton scattering there is a finite probability that a photon after having deposed more than 20 keV energy in one detector leaves again some energy in another detector creating what in the following we will call "double hit". For 25 U/Si layers module from our Monte Carlo simulation we have found that the probability that an incoming photon produces a double hit event is about 8.5 %. In this case we used as detection coordinates, the coordinates corresponding

to the energy deposition in the silicon detector nearest to the volume of interest. This choice is justified by the consideration that the gamma scattered forward and therefore having a greater energy compared with a backscattered photon, has a bigger probability to cause a double event. From our Monte Carlo simulation we evaluated that the number of double hit events with a backscattered photon is the 23% of the total number of double hit events i.e. the 2 % of the total count rate. However, due to the detector module geometry, a backscattered photon has a 90% probability to produce an event in the second detector hitted with the same coordinates as in the first one. We can finally estimate that only 0.2 % of the incoming photon will contribute to decrease image contrast because of the incorrect recognition of the first hitted detector.

As final result of the complete simulation the Monte Carlo code produce an output file in which are listed the detection coordinates for the case that both gammas of the annihilation couple have been detected. This case occurs with a coincidence efficiency of 5.8 % .

4. Count rate of the tomograph

Since the PET technique relies on the detection of the coincidence of the two annihilation gammas, it is use to introduce a figure of merit F, which is valid for any coincidence system with two equal detectors, defined as :

$$F = \frac{\varepsilon^2}{\tau} \qquad (1)$$

where ε is the efficiency of a detection module and τ is the resolving time of the electronic coincidence.

Assuming that the solid angle fraction f_Ω subtended at the source is the same for both detectors and the efficiency ε for 511 keV is constant within the solid angle, one can write

$$N_1 = N_2 = 2Sf_\Omega\varepsilon \qquad (2)$$

where N_1 and N_2 are the single rate of the detectors, S is the source activity; from eq. 2 one can calculate the true coincidence rate T and the accidental one A;

$$T = 2Sf_\Omega\varepsilon^2 \, , \; A = 2N_1N_2\tau \qquad (3)$$

In terms of T and A, F finally becomes

$$\frac{\varepsilon^2}{\tau} = 2\frac{T^2}{A}$$

For a given set of detectors T/A is inversely proportional to the source activity :

$$F = \frac{T}{A} = \frac{1}{4Sf_{\Omega}\tau}$$

For our designed tomograph, assuming $f_{\Omega} = 0.04$, $\tau = 30\ 10^{-9}$ sec for a signal to noise ratio equal to 1 we need a source of about $S_{(T/A=1)} = 2\ 10^8$ Bq ($5\ 10^{-3}$ Ci). At this source activity the T rate is equal to $\frac{\varepsilon^2}{\tau}$ that in our case is $8\ 10^5$ count/sec. With a rate like this one can estimate that even taking into account the decreasing of the T rate due to the absorption and scattering in the tissue and the time spent to complete the scan moving the two modules in different angular position, the total time to store data for a good quality image is about few minutes.

5. Results of the image reconstruction

To reconstruct the image of the simulated source we used the Monte Carlo output data as input data for a simple reconstruction program based on 3D-back projection algorithm [16]. We have chosen to structure the region of interest as a cubic volume of 64 x 64 x 64 voxels each one of 0.5 x 0.5 x 0.5 mm^3. The two gamma detection coordinates define the line of flight of the two photons. The reconstruction program assigns to every voxel crossed by this line of flight a constant numerical value, the final image is obtained summing up the contibutions of the whole set of data.

The simulated radioisotope distribution was a ^{18}F pointlike source. In order to simulate the rotation of the modules around the source, thanks to the fact that the source is in the coordinate center and to its radial simmetry, we have simply divided the set of data in subsets and we have applied to each subset a coordinate rotation corresponding to the angular rotation of the real module thus simulating the complete scan.

In fig. 6 we show a radial cut of the reconstructed ^{18}F pointlike source. This histogram indicate clearly that we have obtained about 2 mm (FWHM) resolution.

In fig. 7 we show a bidimensional lego plot of the same reconstructed distribution corresponding to the central slice of the volume of interest.

6. Conclusion

We have shown that a Positron Emission Tomograph based on the use of multistrip multilayer Si/U detectors can reach 2 mm (FWHM) spatial resolution for a pointlike F-18 source.

The overall complexity of the designed tomograph looks compatible with up to date technology in silicon detector calorimetry. Moreover, the cost and the simplicity of use of a tomograph like the one we designed look appeling for medical use.

Increasing the number of detectors, thus increasing the overall complexity, one could get a even greater efficiency and/or a greater solid angle coverage.

This Monte Carlo study, therefore, encourages further Monte Carlo studies and experimental test to exploit the use of silicon detectors in Positron Emission Tomography.

Acknowledgement

One of us (C.R.) thanks A. Del Guerra for having introduced him to the field of Positron Emission Tomography.

References

1. A. Del Guerra. "Physics and instrumentation in Positron Emission Tomography", Physica Medica - Vol III, Supplement 1 (1992) 35.
2. E.R. Wrenn, M.L. Good and P. Handler. "The use of Positron Emitting Radioisotopes for the localization of brain tumours", Sci. **113** (1951) 525.
3. W.H. Sweet. "Uses of Nuclear Disintegration in the Diagnosis and treatment of brain tumours", New. Engl. J. Med. **245** (1951) 875.
4 Brownell GL, Sweet WH. "Localization of brain tumours with positron emitters". Nucleonics 1953 : 11; 40.
5. E. Browne and R.B. Firestone. "Table of Radioactive Isotope", edited by V.S. Shirley, (John Wiley & Sons, New York, 1986).
6. S.E. Derenzo. "Precision Measurements of annihilation point spread function for medically important positron emitters", in Positron Annihilation, edited by R.R. Hasiguti and K. Fujiwara, (Japan Institute of Metals, Sendai, Japan, 1979); 819.
7. P.Colombino, B.Fiscella and L.Trossi. "Study of positonium in Water and Ice from 22 to -144 °C by Annihilation Quanta Measurements", Nuovo Cimento **38** (1965) 597.
8. Thompson C.J., Yamamoto Y.L., Meyer E.. "PositomeII : a high efficiency positron imaging system for dynamic brain studies. IEEE Trans. Nucl. Sci. 1979 : NS-26; 583.
9. A.Del Guerra et al., "Test of the HISPET prototype", IEEE NS-37, April 1990, 817.
10. M.Bocciolini et al., "A silicon imaging calorimeter prototype for antimatter search in space : experimental results", Nucl. Inst. and Meth. **A333** (1993) 560.
11. see e.g. G.Anzivino et al.; Nucl. Inst. and Meth. **A256** (1987) 65.
12. G. Batignani et al., Nucl. Phys. B (Proc. Suppl.), **23B** (1991) 291.
13. M. Conti et al., "Use of a Transputer network in Digital Radiography", Physica Medica - Vol. IX, Supplement 1 (1993) 239.
14. F.Arfelli et al., "SYRMEP (SYnchrotron Radiation for MEdical Physics). Performance of the digital detection system", Physica Medica - Vol. IX, Supplement 1 (1993) 229.
15. R. Brun et al., "GEANT User's Guide", CERN-DD-EE **81-1** (1991).
16. C.Rizzo, M.Conti, A.del Guerra, "Evaluation of the imaging capabilities of HISPET", Phys. Med. 1987 : 1, 19.

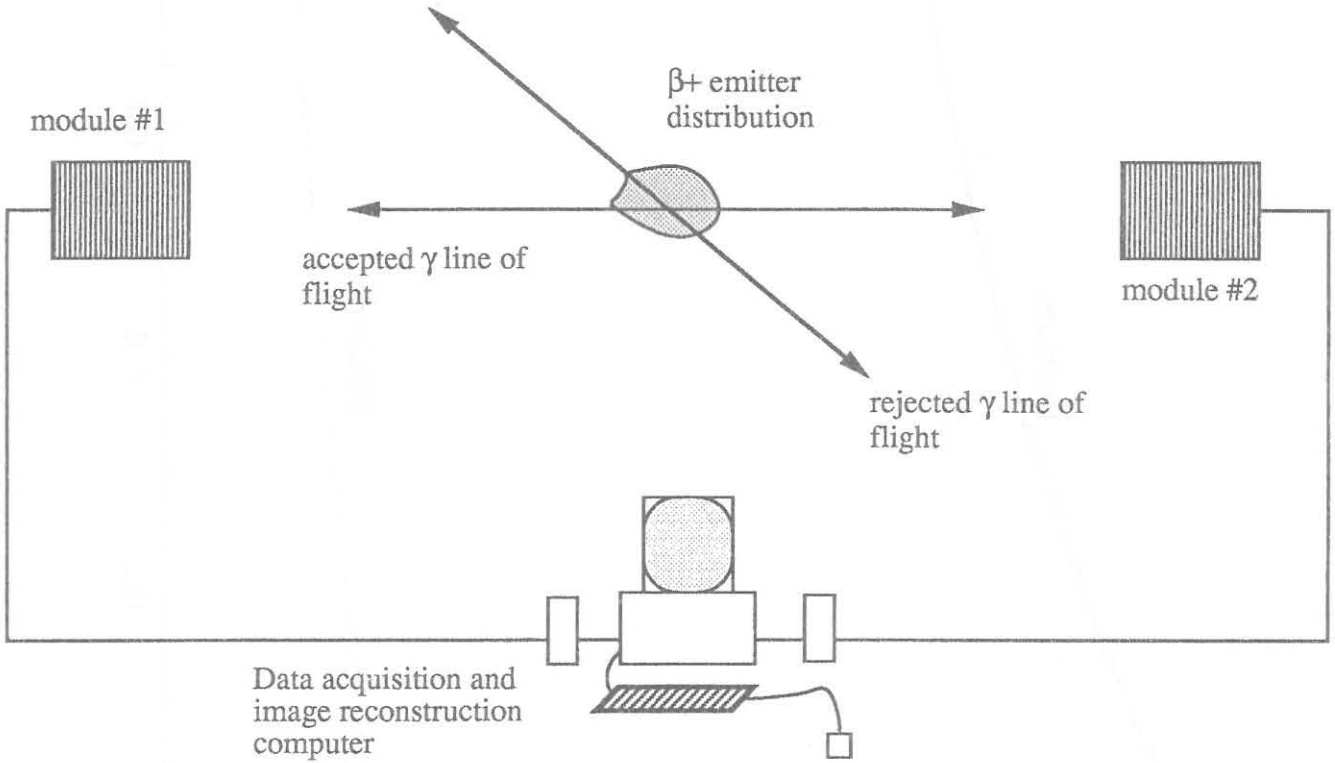

Fig. 1 - Schematic drawing of the simulated tomograph.

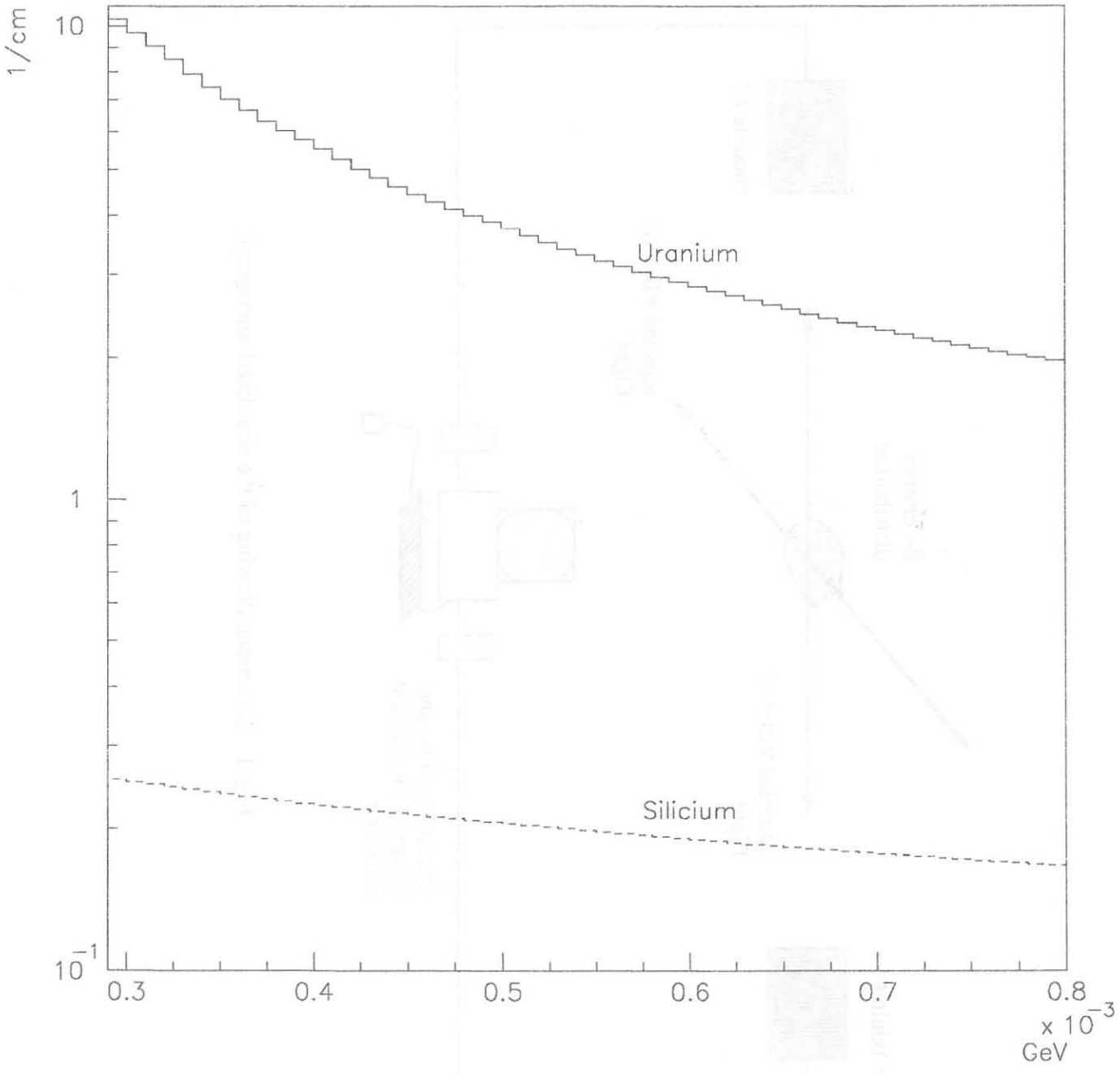

Fig. 2 - Photon cross sections for U and Si.

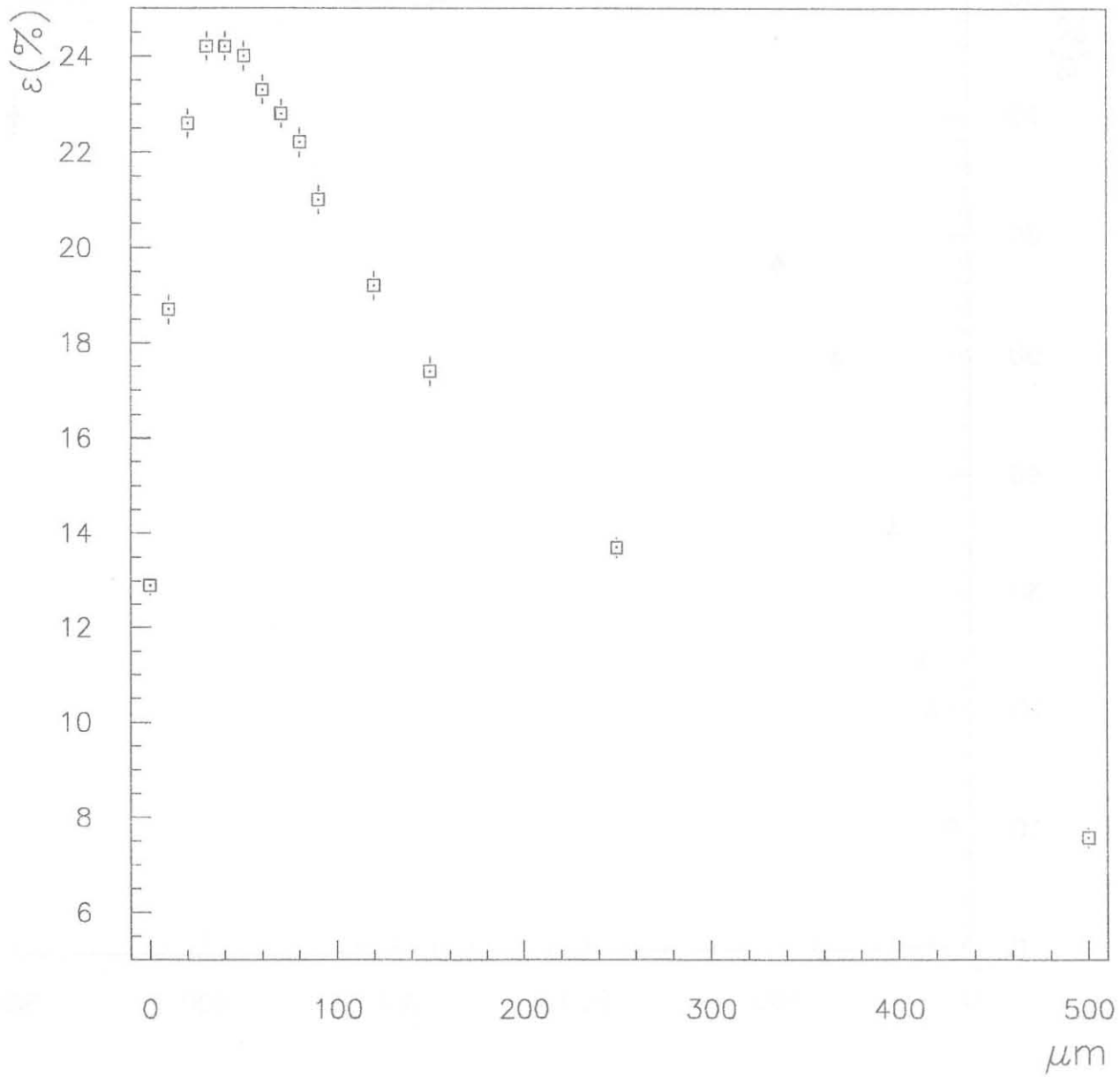

Fig. 3 - Detector efficiency vs Uranium converter thickness per Si detector for 25 detector layers.

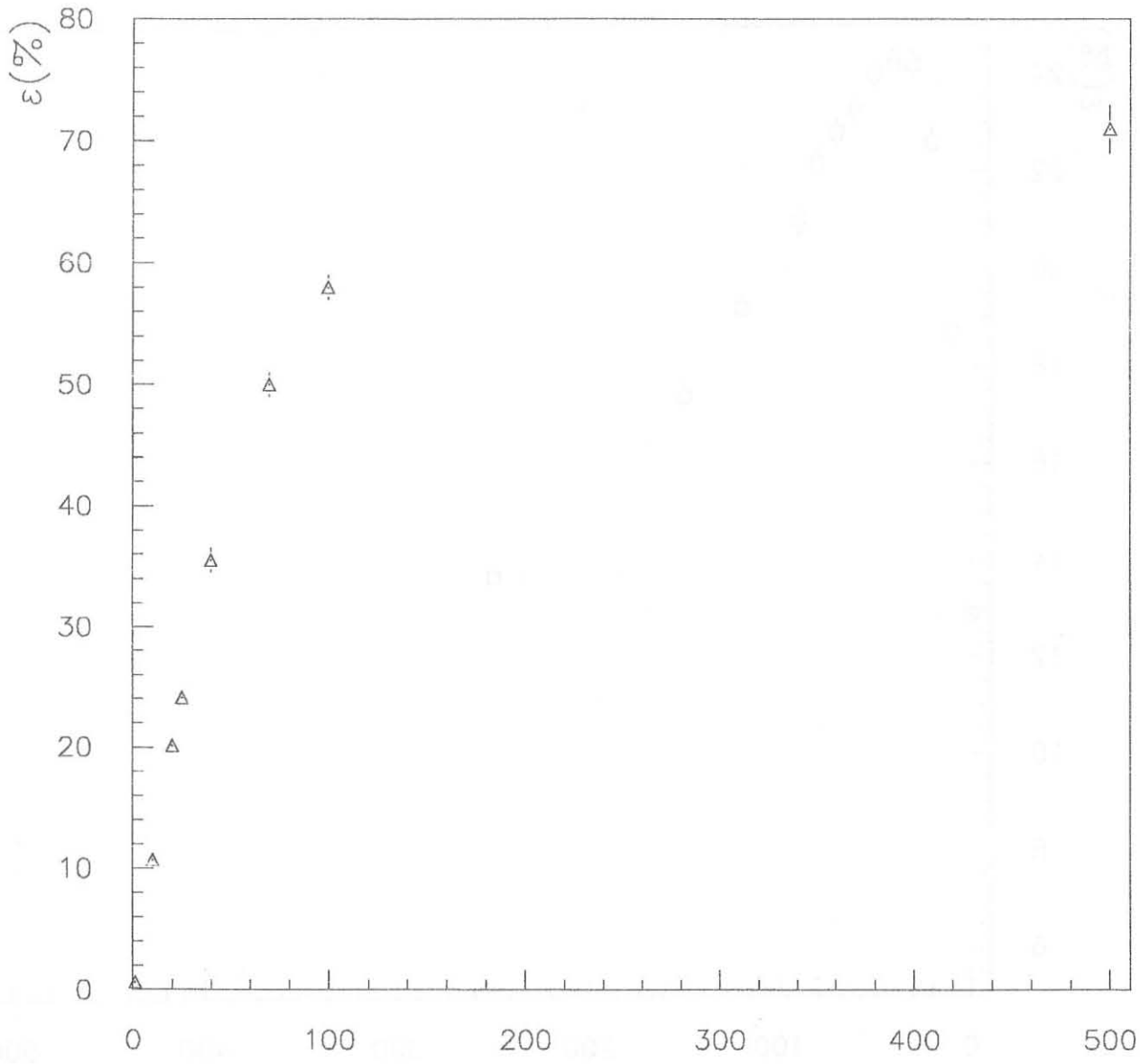

Fig. 4 - Detector efficiency vs number of U/Si layers for 40 μm of U per Si detector.

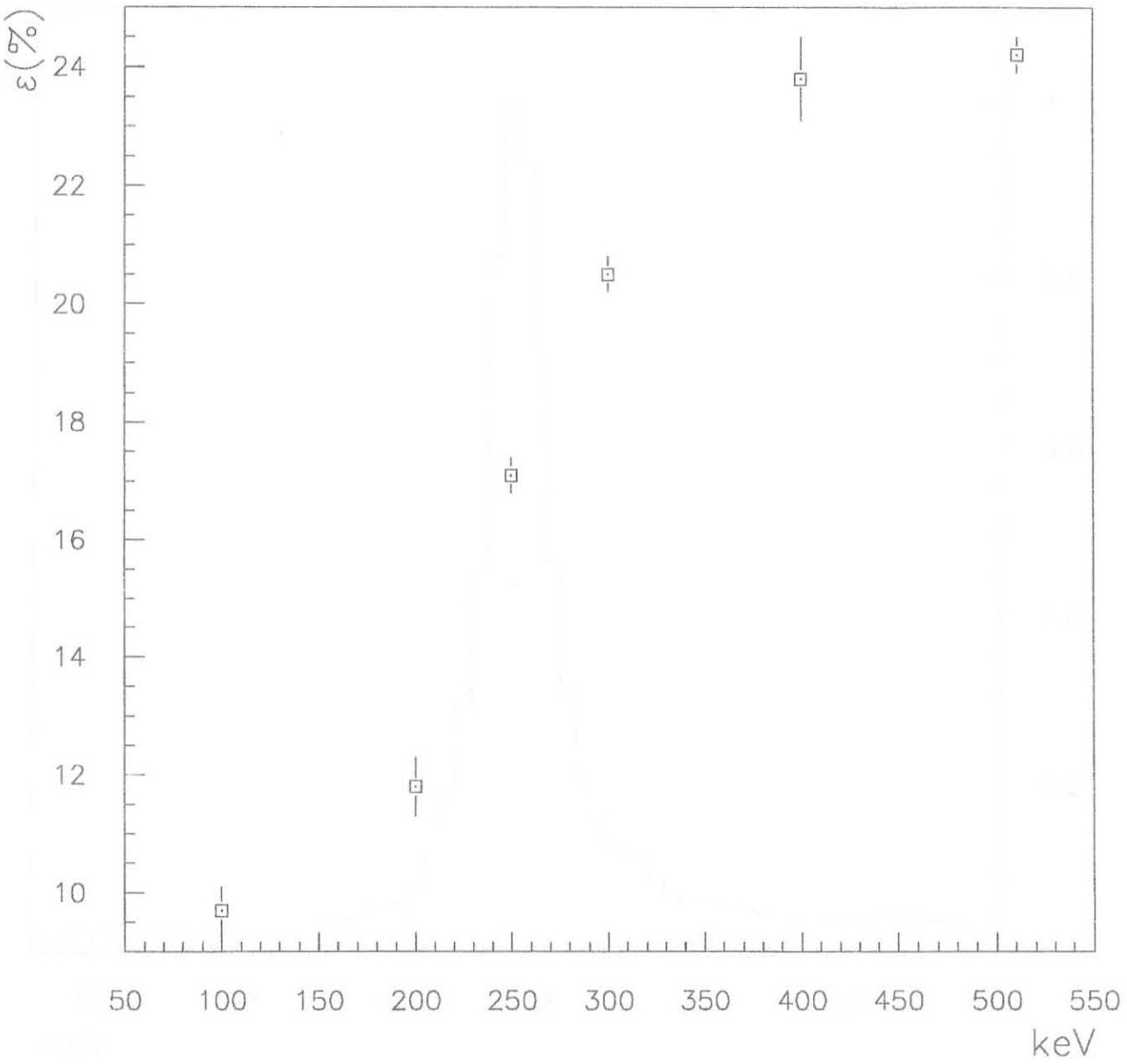

Fig. 5 - Efficiency for a 25 U/Si layer module vs gamma energy.

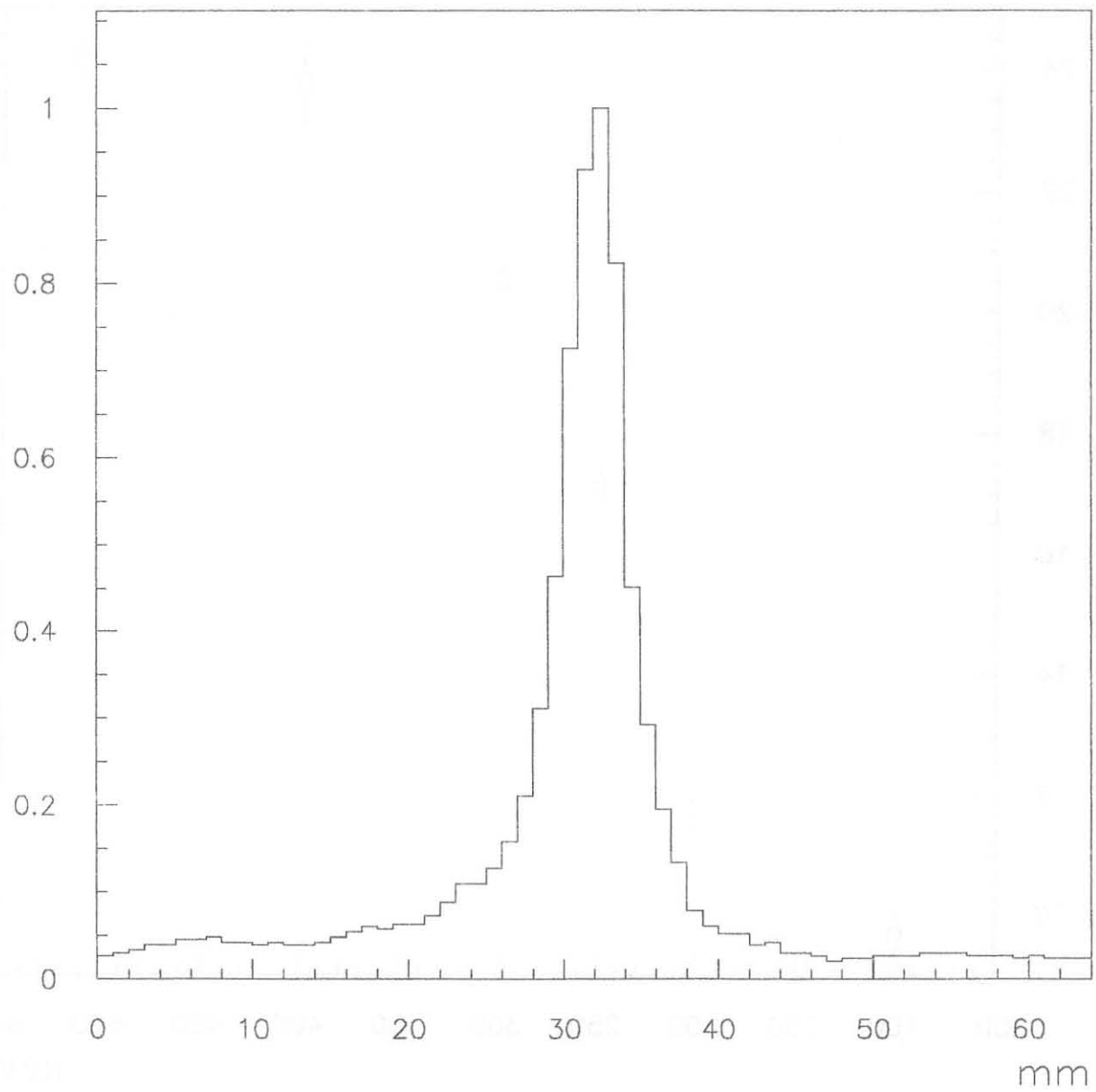

Fig. 6 - Radial cut of the reconstructed ^{18}F pointlike source.

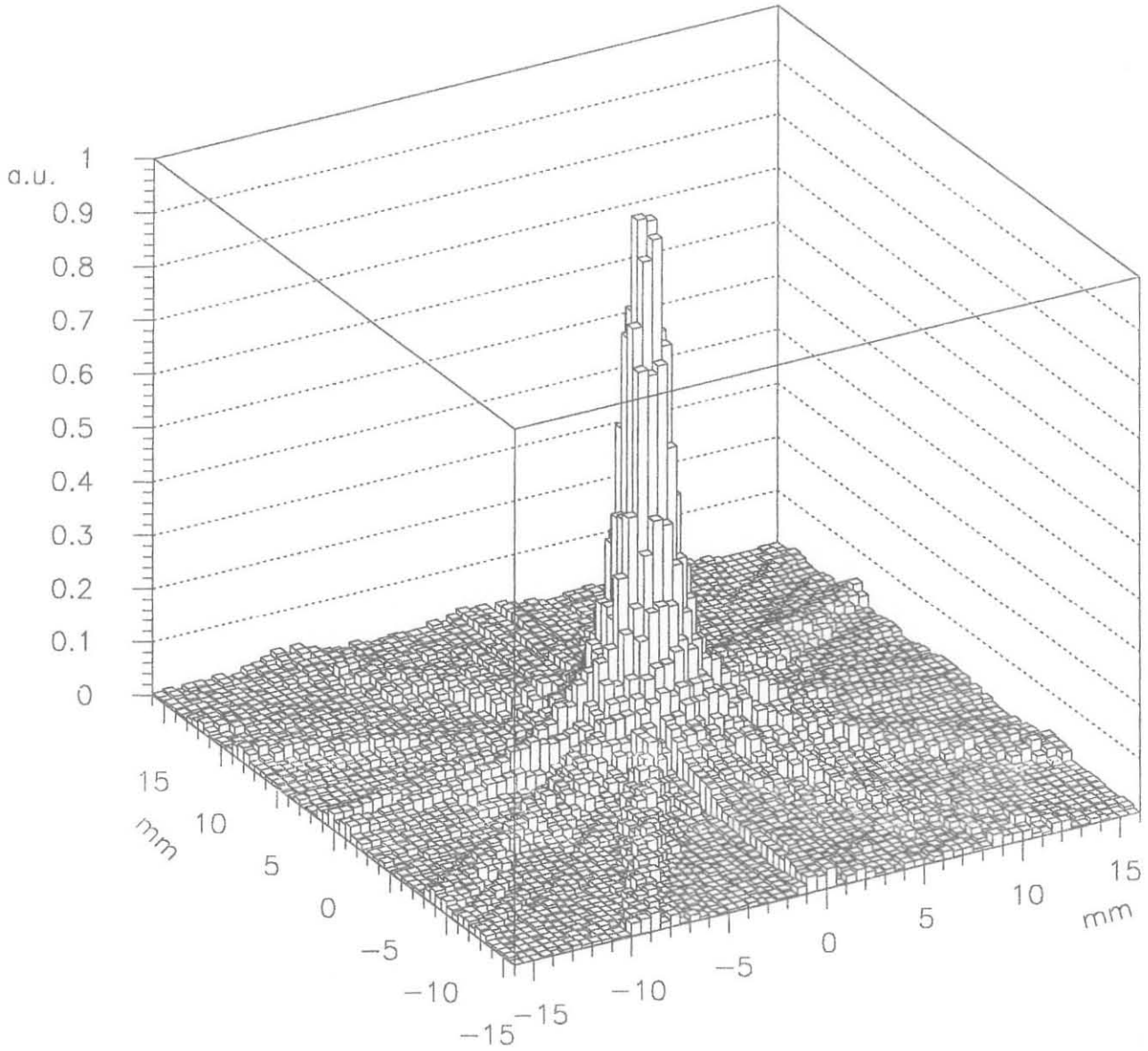

Fig 7 - Lego plot of the central slice of the volume of interest.